

Silencing of *NUF2* inhibits proliferation of human osteosarcoma Saos-2 cells

H.-L. FU, L. SHAO

Department of Orthopaedic Surgery, the Second Affiliated Hospital of Harbin Medical University, Harbin, Heilongjiang, China

Abstract. – OBJECTIVE: *NUF2* (*NUF2*, Ndc80 kinetochore complex component), which is essential for kinetochore-microtubule attachment in mitosis, has emerged as a critical mediator of the cell cycle in multiple tumour occurrences. In the present study, we aimed to investigate the role of *NUF2* in osteosarcoma, one of the most common primary bone tumours in children and young adults.

MATERIALS AND METHODS: Lentivirus-mediated short-hairpin RNA (shRNA) targeting *NUF2* (Lv-sh*NUF2*) was employed for evaluation in human osteosarcoma Saos-2 cells. After *NUF2* silencing, the proliferation of Saos-2 cells was significantly inhibited, as determined by the MTT assay.

RESULTS: The colony forming ability was also significantly decreased in Saos-2 cells infected with Lv-sh*NUF2*. Flow cytometry revealed that downregulation of *NUF2* in Saos-2 cells caused a remarkable accumulation of the cell population in the S phase. Furthermore, the expression levels of cell cycle regulators cyclin A and cyclin-dependent kinase 2 (CDK2) were notably decreased, whereas those of cyclin-dependent kinase inhibitors p21Cip1 and p27Kip1, were increased in response to *NUF2* knockdown in Saos-2 cells.

CONCLUSIONS: Our findings suggest that *NUF2* might modulate cell proliferation via cell cycle control in Saos-2 cells. Downregulation of *NUF2* by shRNA might be a novel strategy for early treatment of osteosarcoma using molecular-targeting therapy.

Key Words:

NUF2, Short-hairpin RNA, Proliferation, Cell cycle, Osteosarcoma.

DMEM = Dulbecco's modified Eagle's medium; FBS = fetal bovine serum; qPCR = quantitative PCR; PMSF = phenylmethylsulfonyl fluoride; FACS = fluorescence activated cell sorting; CDK = cyclin-dependent kinases.

Introduction

Osteosarcoma (OS) is the most common primary malignant bone tumour in children and young adults¹, characterized by atypical osteoid-producing cells. Its dissemination typically occurs via the bloodstream, primarily targeting the lungs and other bones². Almost all types of OS are high grade and have a poor prognosis, with 10-20% of patients showing detectable metastases to the lungs at the time of diagnosis. For the last few decades, the combination of surgery and chemotherapy has greatly improved the survival rate of patients with localized OS³. However, a significant proportion of OS patients show poor response to treatment, a high risk of local relapse, or distant metastasis⁴. To date, the molecular events that initiate and propagate osteosarcoma genesis remain unclear. Thus, the identification of novel and specific molecular markers is particularly necessary for improvements in the treatment of OS.

Recently, molecular targeting therapy has greatly advanced our knowledge of disease pathogenesis and treatments. Among the different proteins investigated for their association with cancer, the NDC80/*NUF2* complex of proteins is frequently implicated in tumorigenesis⁵. *NUF2* is a kinetochore protein that functions to form a stable complex with SPC24, SPC25, and HEC1 (termed the NDC80 complex). In mitosis, *NUF2*, as well as other NDC80 complex components mainly contribute to kinetochore-microtubule attachment⁶. Current evidence has shown that human *NUF2* potentially interacts with centromere-associated protein E and is essential for

Abbreviation List

shRNA = short-hairpin RNA; CDK2 = cyclin-dependent kinase 2; OS: osteosarcoma; CDCA1 = cell division cycle associated 1; Lv-sh*NUF2* = lentiviral vector system delivering short-hairpin RNA against *NUF2*; CDC2 = cell division cycle 2; GFP: green fluorescent protein;

stable spindle kinetochore-microtubule attachment⁷. Consistently, downregulation of NUF2 blocked stable kinetochore-microtubule attachment and induced mitotic cell death in HeLa cells⁶. In particular, it was predicted that the CH domain of NUF2 is pivotal for NUF2-mediated kinetochore-microtubule attachment in cells⁸.

Notably, NUF2 is also known as cell division cycle associated 1 (CDCA1), which was first identified to be overexpressed in various histological types of lung cancers through genome-wide expression analysis⁹. Moreover, activation of NUF2 is involved in pulmonary carcinogenesis and is associated with patients' prognosis. In another report, NUF2 was identified to be a novel cancer-testis antigen that is overexpressed in various human cancers, including lung, cholangiocellular, renal cell, and urinary bladder cancers. It was even thought to be an ideal tumour-associated antigen useful for both diagnosis and immunotherapy of human cancers¹⁰. In fact, recent findings also reported that siRNA-mediated knockdown of NUF2 also inhibited cell proliferation and induced apoptosis in colorectal and gastric cancers¹¹. These reports shine light on the possible role of NUF2 in human cancer development.

Given all these findings, we aimed to study the role of NUF2 in human OS cell growth. A lentiviral vector system delivering short-hairpin RNA against NUF2 (Lv-shNUF2) was employed in the present study. Because NUF2 was a cell cycle-associated gene that co-expressed with known cell cycle regulators such as cell division cycle 2 (CDC2), topoisomerase II and cyclins¹², we also assessed changes in expression of cell cycle regulators in response to the downregulation of NUF2 in human OS Saos-2 cells.

Materials and Methods

Reagents

The lentiviral vector system expressing green fluorescent protein (GFP) was obtained from Ji Kai Genechem Co. (Shanghai, China). The SuperScript III cDNA reverse transcription kit was purchased from Invitrogen (Carlsbad, CA, USA). Anti-NUF2 primary antibody was purchased from Abcam (Hong Kong, China). Primary antibodies against CDK2, cyclin A, p21Cip1, p27Kip1, and GAPDH were commercially purchased from Santa Cruz Biotechnology (Santa Cruz, CA, USA). For stable ablation of NUF2, specific short-hairpin RNA targeting NUF2

(shNUF2) was obtained from Santa Cruz Biotechnology. A non-targeting shRNA (shCon) was also identified.

Cell Lines and cell Culture

Human OS cell lines, Saos-2, U2OS, MG63, and SF-86 were purchased from Shanghai Institute of Biological Sciences, Chinese Academy of Sciences (Shanghai, China). Cells were all maintained in Dulbecco's modified Eagle's medium (DMEM) (Gibco, Grand Island, NY, USA) supplemented with 10% fetal bovine serum (FBS) (Gibco) at 37°C in a 5% CO₂ humidity-controlled incubator. Culture medium was refreshed every 2 days.

Recombinant NUF2-RNAi-Lentivirus (Lv-shNUF2) Construct

The procedure was carried out as previously described¹³. Induced silent sites were selected from the NUF2 gene using the Ambion short hairpin RNA analysis software (<http://www.invitrogen.com/rnai>). BLAST analysis of the NCBI database (<http://www.pubmed.gov>) further supported that it had no homology with other genes. In total, 5 ml of each complementary oligonucleotide strand (200 μM) and 2 μl of 10×denaturation buffer solution were mixed, and sterilized deionized H₂O was added to obtain a final volume of 20 μl. The reaction mixture was denatured at 95°C for 4 min, and then annealed at room temperature (24°C) for 10 min until it formed double-stranded oligonucleotides (ds-oligo). T4 DNA ligase was used to clone the ds-oligo into the linear vector pGCL-GFP, and the reaction system was built following the manufacturer's instructions. TOPO 10 competent cells of *Escherichia coli* were transformed at room temperature for 5 min, on ice for 30 min, and then spread onto Luria Broth solid medium containing kanamycin. Monoclonal colonies were selected 1 day later and sequenced by TaKaRa (Dalian, China). 293T cells (1 × 10⁵ cells) were transfected with NUF2-RNAi-pGCL-GFP by Lipofectamine 2000 (Invitrogen) according to the manufacturer's instructions. The lentiviral vector was concentrated by low centrifugation at 6000×g for 16 h and resuspended in 1 ml DMEM medium after culturing for 48 h. The lentiviral titre was also determined.

Quantitative Real-Time PCR (qRT-PCR)

Saos-2 cells were transduced with the constructed lentiviruses for 96 h. Subsequently, cells were harvested, and total RNA was extracted using TRI-

zol reagent (Invitrogen, USA). Quality assessment of the RNA sample was first performed by visualizing 28S and 18S rRNA bands by electrophoresis on a 1% gel. Thereafter, RNA was quantified using a NanoDrop 1000 spectrophotometer (Thermo Fisher Scientific, Waltham, MA, USA). cDNA was generated from single-strand mRNA using Superscript VILO™ cDNA Synthesis kits (Invitrogen, USA) following the manufacturer's protocols. Next, quantitative PCR (qPCR) was conducted with the QuantiTect SYBR Green PCR kit (Qiagen, Shanghai, China). PCR cycle conditions were as follows: 95°C for 30 s, 42 cycles of 95°C for 5 s, and 60°C for 32 s. Melting curve analysis was used to evaluate amplification specificity. Data were analysed as previously described¹⁴. β -actin was used as the internal control. The primer sequences used were as follows: *NUF2*: 5'-TAC-CATTCAGCAATTTAGTTACT-3' (forward) and 5'-TAGAATATCAGCAGTCTCAAAG-3' (reverse), β -actin: 5'-CAGAGCCTCGCCTTTGCC-GA-3' (forward) and 5'-ACGCCCTGGTGC-CTGGGGCG-3' (reverse). Data were obtained from experiments performed in triplicate.

Western Blot Analysis

Cultured cells were lysed in ice-cold RIPA buffer supplemented with 1 mmol/l phenylmethylsulfonyl fluoride (PMSF) and 1 μ g/ml aprotinin. Proteins were then quantified using a BCA protein assay kit (Beyotime Biotechnology, Nantong, China). For electrophoresis, equal amounts (30 ng) of proteins were separated on a 12% SDS-PAGE gel for 1.5 h. Subsequently, the proteins were transferred to a polyvinylidene fluoride (PVDF) membrane at a stable voltage for 4 h. Thereafter, the membranes were probed with a specific antibody against *NUF2* at 4°C overnight. Membranes were then washed in TBST three times and incubated with the appropriate HRP-conjugated secondary antibody at room temperature for 1 h. Bands were developed with an Odyssey Infrared Imaging System (Li-Cor Biosciences, Lincoln, NE) using an ECL chemiluminescent solution (Amersham, Pittsburgh, PA, USA).

Cell Viability Assay

The MTT assay was used for cell viability measurement. After lentiviral infection, Saos-2 cells were collected with trypsin and, then, re-suspended to a final density of 6×10^4 cells per ml. Cells were then seeded in a 96-well plate and incubated for 72 h, followed by the addition of 10 μ l of MTT reagent (5 mg/ml). After incubation at 37°C

for 4 h, cell supernatants in each well were removed, and DMSO was then added to dissolve the formazan crystals. The absorbance was determined with a Bio-Rad microplate reader (model 630, USA) at 595 nm. Data were obtained from experiments performed in triplicate.

Colony Formation Assay

To determine the effect of *NUF2* on osteosarcoma genesis *in vitro*, we performed a colony formation assay as previously described in the literature¹⁵. Briefly, after lentiviral infection, Saos-2 cells were seeded into a 6-well plate and cultured at 37°C for roughly 8 days, until most single clones had more than 50 cells. Cells were washed by phosphate buffered saline (PBS), fixed with 4% paraformaldehyde (PFA), and then stained with crystal violet. Images were captured by fluorescence microscopy.

Fluorescence-Activated cell Sorting Analysis (FACS)

To determine the cell cycle distribution of Lv-sh*NUF2*- or Lv-shCon-infected cells, a flow cytometry assay was performed following PI staining as described previously¹⁶. Briefly, Saos-2 cells were harvested and gently re-suspended to generate single-cell suspensions using fluorescence activated cell sorting (FACS) buffer (PBS plus 2% FBS). The cells were then washed with PBS twice, followed by overnight fixation in cold 70% ethanol. After two additional washes with cold PBS, cells were re-suspended in RNase A solution and incubated for 30 min at 4°C. Propidium iodide (PI; 0.05 mg/ml) (Beyotime, Nantong, China) was added to the suspension, followed by incubation at 4°C for 30 min and analysis using a flow cytometer (FACS Cali-bur, BD Biosciences, San Jose, CA, USA).

Statistical Analysis

Data were analysed using SPSS software (version 15.0 for Windows, SPSS Inc., Chicago, IL, USA). Values were expressed as the mean \pm SD from three independent experiments. Statistical analyses were performed using Student's *t*-test. *p* < 0.05 was considered statistically significant.

Results

Expression Levels of *NUF2* in Human OS cell Lines

To study the role of *NUF2* in human OS, we initially observed *NUF2* expression in a set of

OS cell lines. qRT-PCR analysis showed that *NUF2* mRNA was highly expressed in all the four OS cell lines Saos-2, U2OS, MG63, and SF-86, though to some extent, the *NUF2* levels in distinct cell lines seemed to be differential (Figure 1A). Consistently, *NUF2* was amply observed in the selected OS cell lines (Figure 1B), which supports the notion that *NUF2* is overexpressed in OS cell lines. Taken together, our results suggest that *NUF2* is highly expressed in human OS *in vitro*.

NUF2 was Successfully Silenced by Lentivirus-Delivered Short-Hairpin RNA (shRNA)

Based on the results depicted in Figure 1, we employed RNA interference technology to stably silence *NUF2* expression in Saos-2 cells. Short-hairpin RNA targeting *NUF2* (sh*NUF2*) was synthesized and packaged in a lentivirus (Lv-sh*NUF2*). As a control, cells infected with non-targeting shRNA were also used. Infection

efficiency was shown to be approximately 73.3% by fluorescence microscopy (Figure 2A). Then, we conducted qRT-PCR and Western blot analysis to assess *NUF2* knockdown efficiency in Saos-2 cells after infection with Lv-sh*NUF2*. The level of *NUF2* mRNA was significantly decreased in the Lv-sh*NUF2* group while it remained as high as the basal level in the Lv-shCon group (Figure 2B). Furthermore, the protein expression of *NUF2* was barely detectable in Saos-2 cells infected with Lv-sh*NUF2* (Figure 2C). Our data show that an RNA interference lentivirus system that could stably deplete *NUF2* expression in Saos-2 cells was successfully constructed.

Silencing of NUF2 Suppressed Cell Proliferation in Saos-2 cells

The effect of *NUF2* downregulation on OS cell viability was determined by the MTT assay. We found that on day 3, Saos-2 cells infected with Lv-sh*NUF2* presented the lowest proliferative rate. Viable cell numbers in the Lv-sh*NUF2* group were far below those in the Lv-shCon group, at roughly 66% on day 3 and 47% on day 5 (Figure 3, $p < 0.001$). These data strongly suggest that downregulation of *NUF2* in Saos-2 cells significantly reduced the cell proliferation rate and thus inhibited cell growth.

Silencing of NUF2 Inhibited Colony Formation of Saos-2 Cells

To further assess the capability of cell growth in an anchorage-independent condition, we adopted a colony formation assay which is closely related to the *in vivo* condition¹⁷. Colonies were all observed through crystal violet staining, bright field microscopy, fluorescence microscopy, and 6-well plate microscopy (Figure 4A). Results showed that colony size was notably smaller and colony numbers were markedly fewer than observed in control groups. Determination of colony numbers also confirmed that only an average of 13.3 colonies formed in the Lv-sh*NUF2* group, whereas approximately 113 colonies formed in the Lv-shCon group (Figure 4B). Our data reinforce the notion that silencing of *NUF2* significantly inhibits cell growth in Saos-2 cells.

Downregulation of NUF2 Caused Cell Cycle Arrest in Saos-2 cells

NUF2 is a key mediator of kinetochore-microtubule attachment. To assess whether inhibition

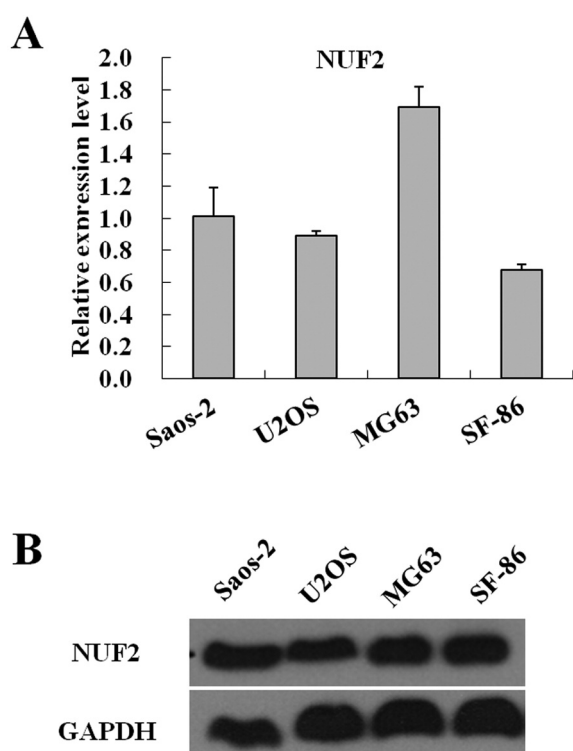


Figure 1. Expression levels of *NUF2* in human osteosarcoma cell lines. qRT-PCR (**A**) and western blot (**B**) analysis of *NUF2* expression in osteosarcoma cell lines Saos-2, U2OS, MG63, and SF-86.

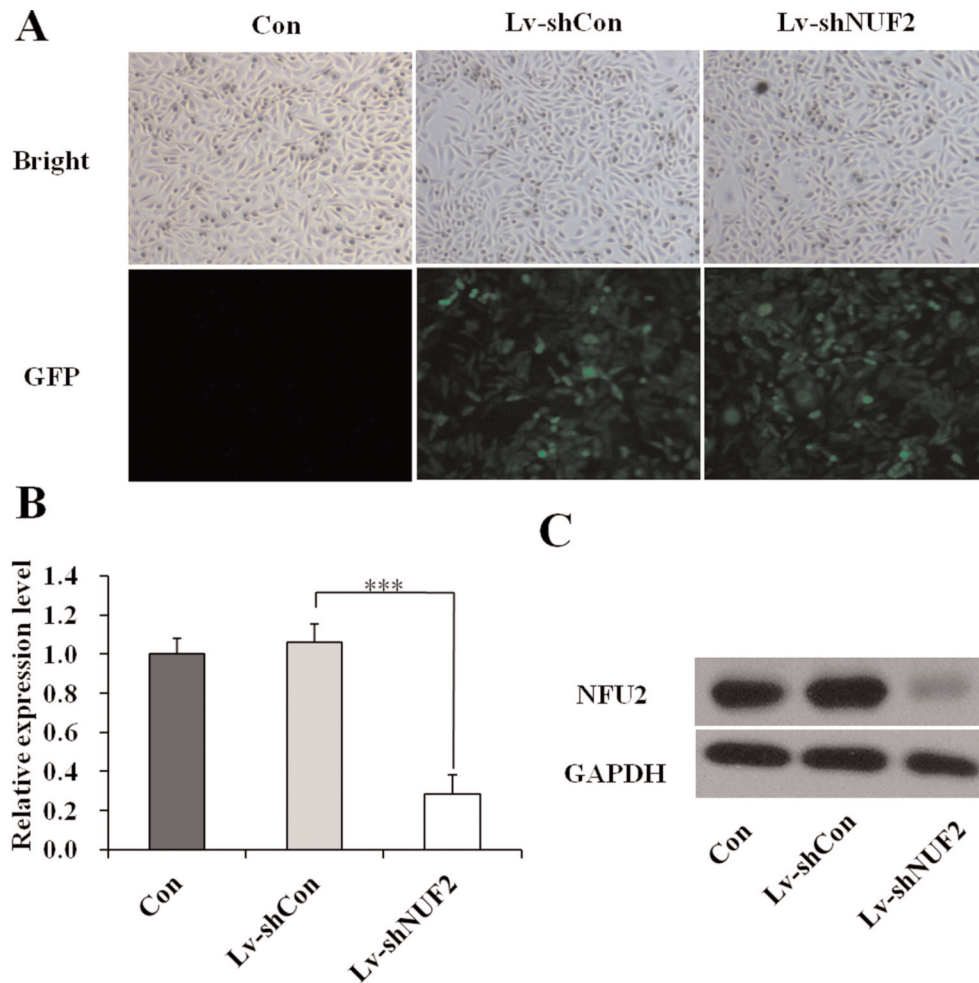


Figure 2. Construction of lentivirus stably expressing shRNA targeting *NUF2*. **(A)** Efficiency of lentiviral infection was reflected by the green fluorescence of GFP. Over 70% cells were GFP positive in both Lv-shCon and Lv-shNUF2 groups. **(B)** qRT-PCR analysis verifying that *NUF2* mRNA expression was successfully depleted by Lv-shNUF2. **(C)** Western blot analysis showing that *NUF2* expression was knocked-down in Saos-2 cells after infection with Lv-shNUF2. ***, $p < 0.001$

of cell growth is linked to cell cycle arrest, we performed flow cytometry to quantify cell proportion in distinct cell cycle phases (Figure 5A). After cell sorting, the cell percentage of each phase was presented for the three groups. We found that after downregulation of *NUF2* in Saos-2 cells, cells were significantly accumulated in the S phase with a notable decrease of cell proportion in the G0/G1 phase (Figure 5B), indicating that downregulation of *NUF2* caused cell cycle arrest at the S phase.

Silencing of NUF2 Down-Regulated CDK2 and cyclin A and up-regulated P21 and P27 in Saos-2 cells

The cell cycle is strictly controlled by cyclins and cyclin-dependent kinases (CDK). In

view of the S phase arrest after *NUF2* down-regulation, we detected the critical G1/S phase regulator CDK2. Meanwhile, CDK2 is also under the regulation of other proteins such as cyclin A or cyclin E and CDK inhibitors p21Cip1 and p27Kip1¹⁸. Western blot analysis was further performed to determine whether these molecules were altered in response to *NUF2* down-regulation. As shown in Figure 6, cyclin A and CDK2 were significantly down-regulated in the Lv-shNUF2 group as compared with the control groups. On the contrary, CDK2 inhibitors p21Cip1 and p27Kip1 were up-regulated in response to *NUF2* depletion. These results suggest that depletion of *NUF2* could block cell cycle progression via suppression of cell cycle regulators.

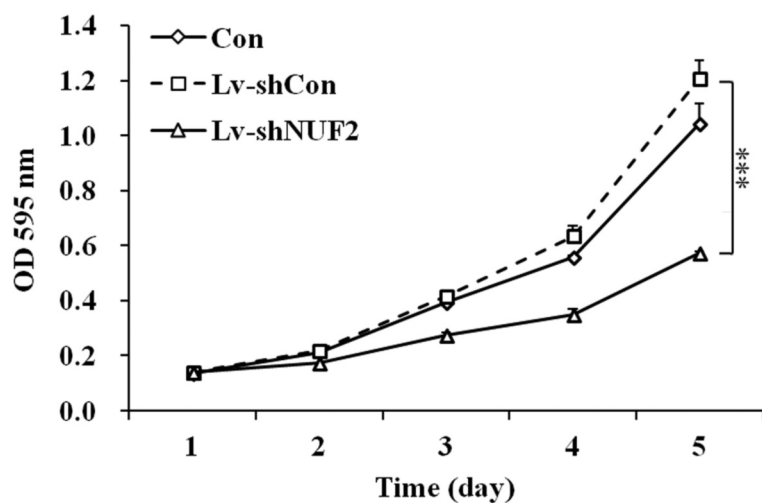


Figure 3. NUF2 downregulation inhibits proliferation of Saos-2 cells. MTT assay showing a significant decrease in viable cell numbers in the Lv-shNUF2 group compared with the control groups. ***, $p < 0.001$

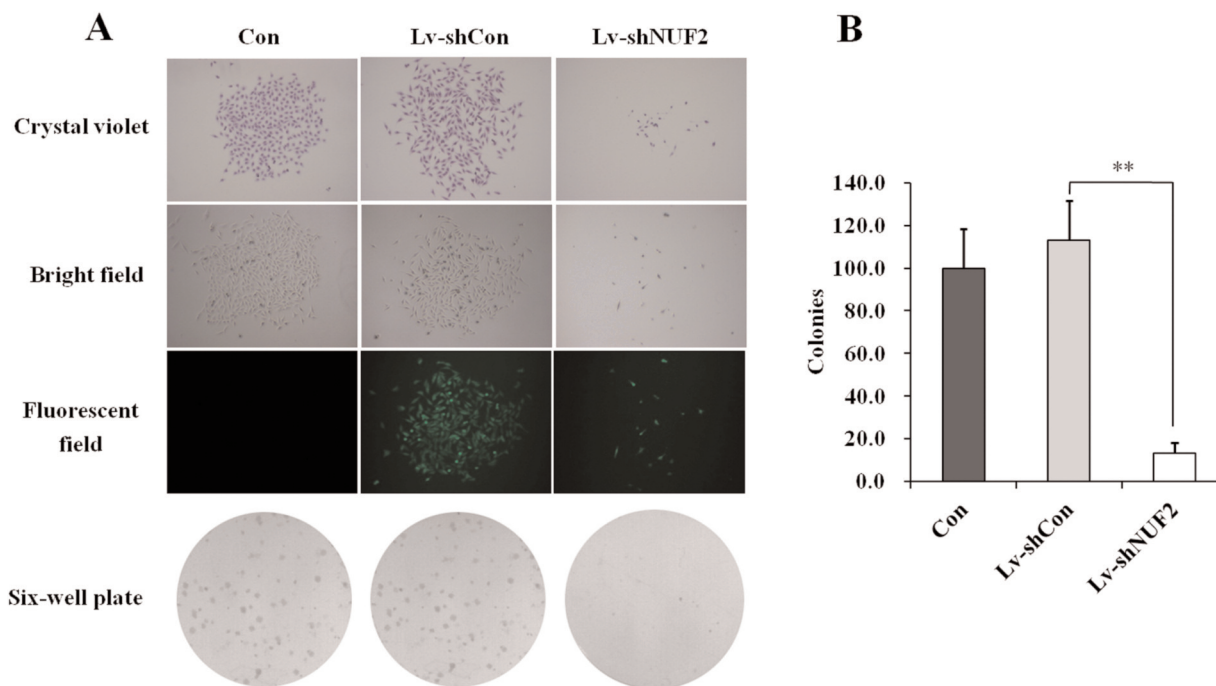


Figure 4. NUF2 downregulation inhibits colony formation of Saos-2 cells. **(A)** Representative photographs of single colony and total colonies in plates are shown. **(B)** Colony counting indicating that NUF2 downregulation significantly lowered the number of colonies of Saos-2 cells. **, $p < 0.01$

Discussion

OS is genetically highly unstable. Current therapeutic strategies are now complicated by chemoresistance and tumour recurrence. Moreover, the low prevalence of OS and its large tumour heterogeneity contribute to the difficulty in achieving meaningful progress in increasing patient survival

rate¹⁹. Since genetic alterations are always implicated in tumorigenesis²⁰, understanding the molecular mechanisms involved in the initiation and development of OS is critical for identifying novel avenues for cancer therapies.

In the present work, we systemically studied the role of NUF2 in human OS cell growth. With the aid of a lentiviral system, we successfully

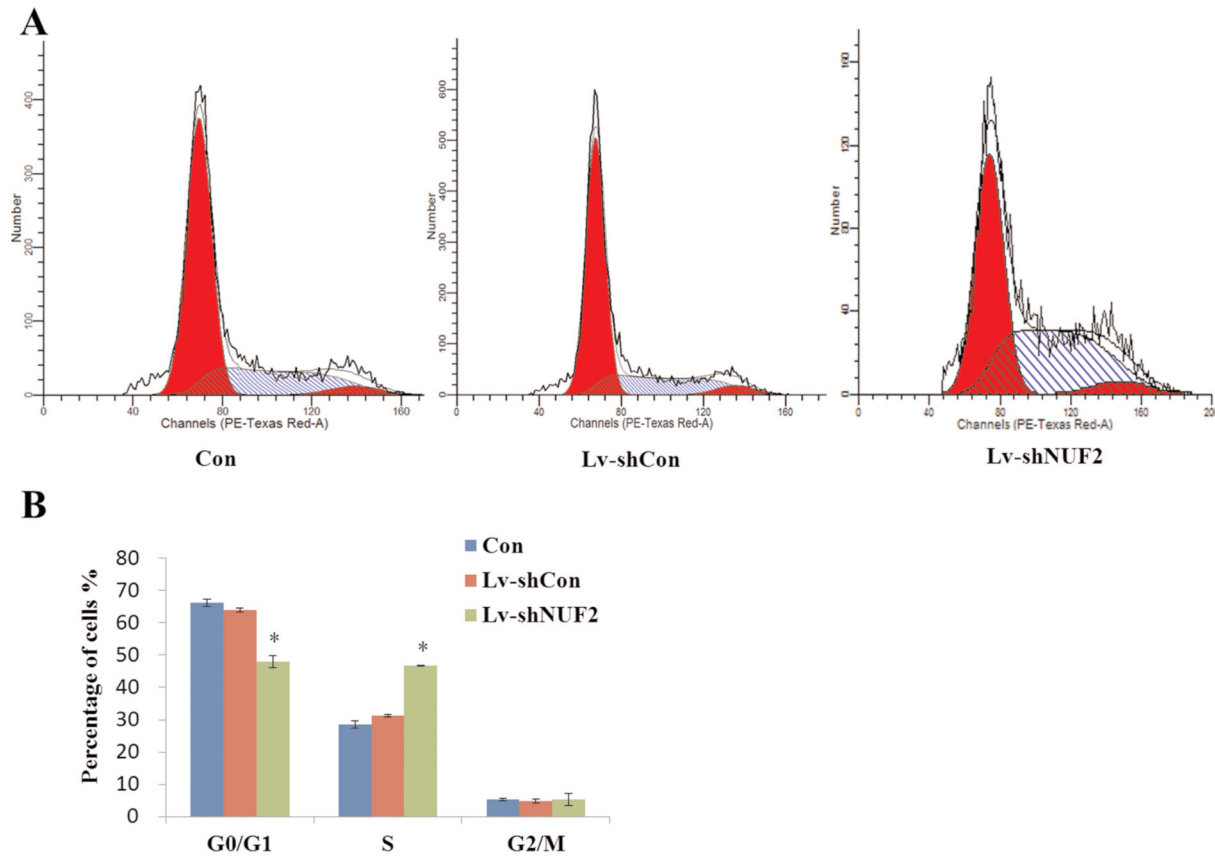


Figure 5. Downregulation of *NUF2* arrests cell cycle progression in Saos-2 cells. **(A)** Cell cycle progression was assayed by flow cytometry in three groups (Con, Lv-shCon, and Lv-shNUF2). **(B)** FACS results showing that Saos-2 cells were more inclined to redistribute in the S phase when infected with Lv-shNUF2. *, $p < 0.05$

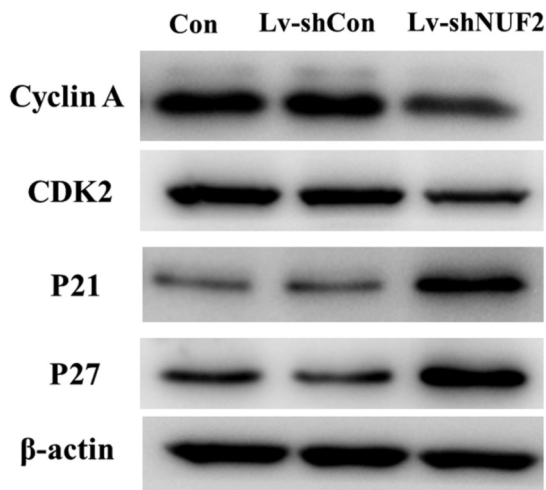


Figure 6. Silencing of *NUF2* down-regulates CDK2 and cyclin A expression and up-regulates p21Cip1 and p27Kip1 expression in Saos-2 cells. Western blot analysis showing the expression changes of cell cycle-related regulators.

downregulated *NUF2* expression in Saos-2 cells. Based on the stable knockdown of *NUF2* in Saos-2, we thereafter aimed to uncover the effects of *NUF2* depletion on Saos-2 cell proliferation and colony formation, which reflect the ability for cell growth. The MTT assay showed that depletion of *NUF2* slowed cell proliferation. The colony formation assay, which is closely related to the *in vivo* situation, was conducted to assess the colony forming ability of *NUF2*-depleted cells. Consistent with the observation with cell proliferation, colony formation was significantly impaired after *NUF2* downregulation. All these data suggest that cell growth was significantly inhibited by *NUF2* depletion. To further uncover the mechanisms underlying the inhibited cell growth, we assessed the cell cycle progression of Saos-2 cells after *NUF2* silencing. We found that the percentage of cells in the G0/G1 phase was notably decreased, whereas cells were mostly accumulated in the S

phase. Western blot analysis further confirmed that the expression levels of cyclin A and CDK2 were decreased, while those of CDK inhibitors p21Cip1 and p27Kip1 were increased. Taken together, all these findings confirmed that NUF2 promotes OS proliferation through regulation of the cell cycle, particularly the G1/S checkpoint.

Identification of NUF2 as a critical mediator in OS cell growth is of great importance. NUF2 has been implicated in a number of human tumorigenesis, including lung, cholangiocellular, renal cell, and urinary bladder cancers¹⁰. However, to our knowledge, the role of NUF2 in OS is still unexamined. Our report may provide evidence to support that NUF2 also plays a critical role in OS cell growth. More importantly, the identification of NUF2 as a pivotal mediator for OS cell growth may provide novel clues for OS treatment and prevention.

One interesting question that arose from our study is why the depletion of NUF2 caused significant cell accumulation in the S phase instead of the M phase. Current evidence has shown that human NUF2 could interact with centromere-associated protein E and is essential for stable spindle kinetochore-microtubule attachment⁷. To date, the knowledge of NUF2 is limited to M phase regulation. However, in our report, we found that it was the G1/S checkpoint in mitosis interphase, instead of the G2/M checkpoint in cell division that was interrupted after NUF2 downregulation. Our results might imply that in addition to the G2/M phase, NUF2 may also be involved in the G1/S transition. However, the detailed mechanism by which NUF2 regulates G1/S transition needs to be examined more thoroughly.

Conclusions

We identified NUF2 as a critical mediator for OS cell growth. Downregulation of NUF2 in Saos-2 cells led to inhibition of proliferation and colony formation, which could be attributed to S phase cell cycle arrest. Our findings provide novel evidence to support the proposal that molecular therapy targeting NUF2 be considered for OS treatment and prevention.

Acknowledgements

This research was supported by grants from the Natural Science Foundation of Heilongjiang Province (No. H2013107).

Conflict of Interest

The Authors declare that they have no conflict of interests.

References

- 1) WANG W, WANG ZC, SHEN H, XIE JJ, LU H. Dose-intensive versus dose-control chemotherapy for high-grade osteosarcoma: a meta-analysis. *Eur Rev Med Pharmacol Sci* 2014; 18: 1383-1390.
- 2) SHWEIKEH F, BUKAVINA L, SAEED K, SARKIS R, SUNEJA A, SWEISS F, DRAZIN D. Brain metastasis in bone and soft tissue cancers: a review of incidence, interventions, and outcomes. *Sarcoma* 2014; 2014: 475175.
- 3) LO WW, PINNADUWAGE D, GOKGOZ N, WUNDER JS, ANDRULIS IL. Aberrant hedgehog signaling and clinical outcome in osteosarcoma. *Sarcoma* 2014; 2014: 261804.
- 4) BACCI G, BRICCOLI A, ROCCA M, FERRARI S, DONATI D, LONGHI A, BERTONI F, BACCHINI P, GIACOMINI S, FORNI C, MANFRINI M, GALLETI S. Neoadjuvant chemotherapy for osteosarcoma of the extremities with metastases at presentation: recent experience at the Rizzoli Institute in 57 patients treated with cisplatin, doxorubicin, and a high dose of methotrexate and ifosfamide. *Ann Oncol* 2003; 14: 1126-1134.
- 5) CHEERAMBATHUR DK, GASSMANN R, COOK B, OEGEMA K, DESAI A. Crosstalk between microtubule attachment complexes ensures accurate chromosome segregation. *Science* 2013; 342: 1239-1242.
- 6) DELUCA JG, MOREE B, HICKEY JM, KILMARTIN JV, SALMON ED. hNuf2 inhibition blocks stable kinetochore-microtubule attachment and induces mitotic cell death in HeLa cells. *J Cell Biol* 2002; 159: 549-555.
- 7) LIU D, DING X, DU J, CAI X, HUANG Y, WARD T, SHAW A, YANG Y, HU R, JIN C, YAO X. Human NUF2 interacts with centromere-associated protein E and is essential for a stable spindle microtubule-kinetochore attachment. *J Biol Chem* 2007; 282: 21415-21424.
- 8) SUNDIN LJ, GUIMARAES GJ, DELUCA JG. The NDC80 complex proteins Nuf2 and Hec1 make distinct contributions to kinetochore-microtubule attachment in mitosis. *Mol Biol Cell* 2011; 22: 759-768.
- 9) HAYAMA S, DAIGO Y, KATO T, ISHIKAWA N, YAMABUKI T, MIYAMOTO M, ITO T, TSUCHIYA E, KONDO S, NAKAMURA Y. Activation of CDCA1-KNTC2, members of centromere protein complex, involved in pulmonary carcinogenesis. *Cancer Res* 2006; 66: 10339-10348.
- 10) HARAO M, HIRATA S, IRIE A, SENJU S, NAKATSURA T, KOMORI H, IKUTA Y, YOKOMINE K, IMAI K, INOUE M, HARADA K, MORI T, TSUNODA T, NAKATSURU S, DAIGO Y, NOMORI H, NAKAMURA Y, BABA H, NISHIMURA Y. HLA-A2-restricted CTL epitopes of a novel lung cancer-associated cancer testis antigen, cell division

- cycle associated 1, can induce tumor-reactive CTL. *Int J Cancer* 2008; 123: 2616-2625.
- 11) KANEKO N, MIURA K, GU Z, KARASAWA H, OHNUMA S, SASAKI H, TSUKAMOTO N, YOKOYAMA S, YAMAMURA A, NAGASE H, SHIBATA C, SASAKI I, HORII A. siRNA-mediated knockdown against CDCA1 and KNTC2, both frequently overexpressed in colorectal and gastric cancers, suppresses cell proliferation and induces apoptosis. *Biochem Biophys Res Commun* 2009; 390: 1235-1240.
 - 12) WALKER MG. Drug target discovery by gene expression analysis: cell cycle genes. *Curr Cancer Drug Targets* 2001; 1: 73-83.
 - 13) ZHAO X, MA C, CAI X, LEI D, LIU D, XU F, JIN T, LIU J, PAN X. RNA interference of caveolin-1 via lentiviral vector inhibits growth of hypopharyngeal squamous cell carcinoma FaDu cells In Vitro and In Vivo. *Asian Pac J Cancer Prev* 2011; 12: 397-401.
 - 14) LI LL, XUE AM, LI BX, SHEN YW, LI YH, LUO CL, ZHANG MC, JIANG JQ, XU ZD, XIE JH, ZHAO ZQ. JMJD2A contributes to breast cancer progression through transcriptional repression of the tumor suppressor ARHI. *Breast Cancer Res* 2014; 16: R56.
 - 15) FRANKEN NA, RODERMOND HM, STAP J, HAVEMAN J, VAN BREE C. Clonogenic assay of cells in vitro. *Nat Protoc* 2006; 1: 2315-2319.
 - 16) CHEN L, GU J, XU L, QU C, ZHANG Y, ZHANG W. RNAi-mediated silencing of ATP-binding cassette C4 protein inhibits cell growth in MGC80-3 gastric cancer cell lines. *Cell Mol Biol (Noisy-le-grand)* 2014; 60: 1-5.
 - 17) WANG LH. Molecular signaling regulating anchorage-independent growth of cancer cells. *Mt Sinai J Med* 2004; 71: 361-367.
 - 18) O'CONNOR PM, FERRIS DK, PAGANO M, DRAETTA G, PINES J, HUNTER T, LONGO DL, KOHN KW. G2 delay induced by nitrogen mustard in human cells affects cyclin A/cdk2 and cyclin B1/cdc2-kinase complexes differently. *J Biol Chem* 1993; 268: 8298-8308.
 - 19) LI B, YE Z. Epigenetic alterations in osteosarcoma: promising targets. *Mol Biol Rep* 2014; 41: 3303-3315.
 - 20) REN XF, MU LP, JIANG YS, WANG L, MA JF. LY21000977761 inhibits metastasis and enhances chemosensitivity in osteosarcoma MG-63 cells. *Eur Rev Med Pharmacol Sci* 2015; 19: 1182-1190.